Title

Preeclampsia and Inflammatory Preterm Labor Alter the Human Placental Hematopoietic Niche

Journal

Reproductive Sciences, 23(9)

ISSN

1933-7191

Authors

Ponder, Kathryn L
Bárcena, Alicia
Bos, Frank L
et al.

Publication Date

2016-09-01

DOI

10.1177/1933719116632926

Peer reviewed

Reproductive Sciences
2016, Vol. 23(9) 1179-1192

DOI: 10.1177/1933719116632926
rs.sagepub.com
SAGE

Preeclampsia and Inflammatory Preterm Labor Alter the Human Placental Hematopoietic Niche

Kathryn L. Ponder, MD[1], Alicia Bárcena, PhD[2], Frank L. Bos, PhD[3], Matthew Gormley, BS[2], Yan Zhou, MD[2], Katherine Ona, MS[2], Mirhan Kapidzic, MD[2], Ann C. Zovein, MD[1,3], and Susan J. Fisher, PhD[2]

Abstract

Background: The human placenta is a source of hematopoietic stem and progenitor cells (HSPCs). The RUNX1 transcription factor is required for the formation of functional HSPCs. The impact of preeclampsia (PE) and preterm labor (PTL, spontaneous preterm labor [sPTL] and inflammatory preterm labor [iPTL]) on HSPC localization and RUNX1 expression in the human placenta is unknown. **Methods:** We compared the frequency and density of HSPC in control samples from sPTL (n = 6) versus PE (n = 6) and iPTL (n = 6). We examined RUNX1 protein and RNA expression in placentas from normal pregnancies (5-22 weeks, n = 8 total) and in placentas from the aforementioned pregnancy complications (n = 5/group). **Results:** Hematopoietic stem and progenitor cells were rare cell types, associated predominantly with the vasculature of placental villi. The HSPC density was greater in the chorionic plate (CP) compared to the villi ($P < .001$) and greater in PE and iPTL samples as compared to controls within the CP (not significant) and overall ($P < .05$). During the fetal period, RUNX1 was expressed in the mesenchyme of the CP and villi. Inflammatory PTL samples were more likely to exhibit intraluminal RUNX1$^+$ cell populations ($P < .001$) and RUNX1$^+$ cell clusters attached to arterial endothelial cells. **Conclusion:** Placental HSPCs likely arise from hematopoietic niches comprised RUNX1$^+$ mesenchyme and vascular endothelium. Pregnancy complications that result in preterm birth differentially affect placental HSPC localization and RUNX1 expression. Our results support previous findings that inflammation positively regulates hematopoiesis. We present new evidence that hemogenic endothelium may be active at later stages of human fetal development in the context of inflammation.

Keywords

human placenta, chorionic plate, hematopoietic stem cells, RUNX1, preterm birth

Introduction

The human placenta is an extraembryonic site of definitive hematopoietic stem cells (HSCs)[1-3] capable of engraftment.[4,5] There is evidence that a portion of these HSCs may develop de novo from the endothelium.[6]

The density of placental HSC peaks in the embryonic period and decreases after 9 weeks of gestation, whereas the total number increases over gestation due to greater placental mass.[1,7] However, the effects of pregnancy pathologies on the frequency, density, and localization of hematopoietic stem and progenitor cell (HSPC) are not known. In this context, understanding the role of the stem cell niche, where HSPCs reside during their development, is important. Previous studies suggest that placental HSPCs reside in mesenchymal and endothelial niches during normal pregnancy.[2,5] The HSPC niche has not been characterized in the setting of pregnancy complications associated with placental pathologies.

Inflammation and preeclampsia (PE) are common etiologies of preterm birth that are associated with short-term hematologic dysfunction in the neonate. One of the most common inflammatory exposures in utero is chorioamnionitis, an

[1] Division of Neonatology, Department of Pediatrics, University of California San Francisco, San Francisco, CA, USA
[2] Department of Obstetrics, Gynecology and Reproductive Sciences, Center for Reproductive Sciences, Eli and Edythe Broad Center of Regeneration Medicine and Stem Cell Research, University of California San Francisco, San Francisco, CA, USA
[3] Cardiovascular Research Institute, University of California San Francisco, San Francisco, CA, USA

Corresponding Author:
Kathryn L. Ponder, Division of Neonatology, Department of Pediatrics, University of California San Francisco, San Francisco, CA 94143, USA.
Email: kathryn.ponder@ucsf.edu

inflammation of the fetal membranes, which is considered an infection if clinical signs are present.[8] Neonates thus exposed are at higher risk for sepsis, thrombocytopenia, and either neutrophilia or neutropenia.[9,10] Preeclampsia is a disorder of shallow placentation and hypoxic stress,[11,12] which is associated with short-term thrombocytopenia and neutropenia in the neonate.[13] Increased platelet and neutrophil consumption, as well as bone marrow suppression, are involved in the underlying pathophysiologies of both conditions. A possible contributing role of the pathological placenta to neonatal hematopoietic dysfunction has yet to be investigated.

The question of altered hematopoiesis is especially important considering the evidence for longer term immune cell dysregulation in preterm infants born due to infection or PE. Chorioamnionitis confers an increased risk for disorders with an underlying component of immune dysregulation, including a 3.6-fold increased risk for cerebral palsy[14,15] and a 4.4-fold increased risk of asthma.[16] Growth restriction is a common neonatal consequence of PE, which increases an individual's risk for developing diabetes or hypertension in adulthood.[17] Evidence of hematologic dysfunction in the setting of placental pathologies could provide insights into these enigmatic associations.

The RUNX1 transcription factor (also known as AML1 or CBFA2) is required for the formation of functional HSCs[18] and is an important regulator of hematopoiesis in the mouse placenta.[6] Aside from low expression levels in trophoblasts reported in the Human Tissue Atlas, RUNX1 has not been studied in the human placenta.[19] This transcription factor is critical for the developmental generation of HSPCs from hemogenic endothelium, which appear as cell clusters associated with the vascular endothelium.[6,18,20-22] RUNX1 is expressed by multiple cellular compartments in human[23] and mouse embryos, which include HSPCs, endothelium, and subvascular mesenchyme.[20,21,24] Similarly, placental RUNX1-lacZ expression in mice is found in association with the intraluminal cells of the labyrinth vasculature, in the endothelial cells lining the chorioallantoic vessels, and in the subvascular mesenchyme.[6,25] RUNX1-lacZ is also expressed in the chorionic plate.[25] Human placental expression of RUNX1 has yet to be characterized in normal pregnancy, and it is unknown whether its expression pattern changes with complications associated with overt placental pathologies.

We hypothesized that RUNX1, as a marker of definitive hematopoiesis, would be expressed in the human placenta and chorionic plate throughout gestation. Characterizing HSC formation in the context of the niche is essential to harvesting and expanding these cells ex vivo for further experimental or clinical use. We also theorized that a subset of pregnancy complications that result in preterm birth would affect the frequency, density, and localization of $RUNX1^+$ cells and HSPCs in the placenta and chorionic plate. In turn, this information could yield insights into the impact of these conditions on the neonatal immune system. The placenta is a readily available hematopoietic organ with tremendous potential for this purpose.

Methods

Patient Population

Placental biopsy specimens were obtained from the University of California, San Francisco (UCSF) tissue bank or at the time of delivery from Moffitt-Long Hospital, UCSF. Samples were from 3 groups of patients who delivered preterm: (1) spontaneous preterm labor with no clinical evidence of inflammation (sPTL); (2) preterm labor with evidence of inflammation (iPTL); or (3) PE.

The sPTL samples, which served as controls, were from patients diagnosed according to previously published criteria.[26] They included regular uterine contractions after 20 weeks or before 37 weeks of gestation that were $\leq$5 to 8 minutes apart and accompanied by one or more of the following: (1) progressive changes in the cervix, (2) cervical dilation of $\geq$2 cm, and/or (3) cervical effacement of $\geq$80%. Preeclampsia and iPTL samples comprised the experimental groups. Clinical laboratory values and pathological findings (from amniocentesis, placental pathology, and reverse transcription/polymerase chain reaction analyses; interleukin 1 and tumor necrosis factor α) or a maternal diagnosis of clinical chorioamnionitis[8] were used to differentiate between inflammatory and noninflammatory PTL. Patients with PE were diagnosed with mild or severe PE or HELLP (Hemolysis, Elevated Liver enzymes, Low Platelet count) syndrome prior to 37 weeks of gestation as described previously.[27]

Samples from 5 to 22 weeks of gestation were from elective pregnancy terminations at San Francisco General Hospital. The gestational ages (GAs) of first-trimester specimens were estimated based on crown-rump lengths, measured by ultrasonography. The GAs of second-trimester specimens were estimated by foot length.

Informed Consent

Tissue bank collection was reviewed and approved by the UCSF Committee on Human Research. The UCSF specimens collected at the time of delivery were obtained using consent forms and procedures that were approved by the same committee.

Immunolocalization and Confocal Fluorescence Microscopy

Freshly collected samples of the chorionic plate and placental villi from UCSF and San Francisco General Hospital were fixed in 4% paraformaldehyde for 90 minutes, infiltrated with 7.5% to 15% sucrose, followed by optimal cutting temperature medium, frozen in an ethanol-dry ice mixture, and stored at -80°C until they were processed. Tissue bank specimens were processed using a similar protocol.

Sections (30 μm) of the fixed/frozen tissue were stained with combinations of the antibodies that are listed in Supplementary Table 1. Dilutions and incubation times/temperatures are also given.

As controls, serial sections were stained with the secondary antibody alone or mouse immunoglobulin G_1-fluorescein isothiocyanate (BD Pharmingen, San Jose, California). Staining with Prolong Gold antifade reagent with 4′ 6-diamidino-2-phenylindole (DAPI; Life Technologies, Rockford, Illinois) was used to visualize nuclei. Slides were imaged on Leica DM 6000 CS and Leica SPE confocal microscopes (Leica Microsystems, Inc, Buffalo Grove, Illinois).

Because confocal microscopy does not afford the discrimination enabled by flow cytometry, we identified HSPCs as $CD34^+CD45^+$ rounded cells.[5] Frequency was calculated as the number of HSPCs per field. For quantifying HSPC density, DAPI-stained nucleated cells were counted using ImageJ,[28] and the number of HSPCs relative to nucleated cells was established. Endothelial cells were identified as $CD34^+CD45^-$, whereas mesenchymal cells were identified as $vimentin^+CD34^-CD45^-$. We profiled RUNX1 mean fluorescence intensity across images from the embryonic stage using ImageJ software.[28]

Detection of RUNX1 RNA Expression by RNA-Seq and Protein Expression by Immunoblotting

RNA-seq data were generated from human placental chorionic villi and smooth chorion samples (n = 2/sample type and trimester) processed in our laboratory as part of the National Institutes of Health (NIH) Roadmap Epigenomics Consortium, as described previously.[29] For immunoblotting experiments, cells from the human placental villous mesenchyme and chorionic plate were isolated as described previously.[1] Proteins were extracted into a lysis buffer containing proteinase inhibitors (Thermo Scientific 1861281, Waltham, Massachusetts) diluted 1:100 in CelLytic (Sigma C2978, Saint Louis, Missouri), then flash frozen in liquid nitrogen, and stored at −80°C until use. Proteins were denatured with 5% β-mercaptoethanol in sodium dodecyl sulfate loading buffer, transferred to nitrocellulose membranes, and overlaid with an RUNX antibody (Clone EPR3099; Abcam, Inc, Cambridge, Massachusetts) diluted 1:100 in blocking buffer (phosphate-buffered saline with 0.25% Tween and 10% nonfat milk) and incubated at 4°C overnight. Binding of peroxidase-conjugated goat antirabbit (1:5000) was used to detect binding of the primary antibody. Actin (1:10 000) served as an internal control. Proteins were visualized with Pierce enhanced chemiluminescence system 2 substrate (Thermo Scientific 80196). It should be noted that although the RUNX antibody (EPR3099) is reported by Abcam to detect overexpression levels of RUNX2 and RUNX3 in immunoblots, hematopoietic niches and cells primarily express RUNX1,[20,24] and hence, we will refer to immunofluorescence with this antibody as RUNX1.

Statistical Analysis

A power analysis was used to estimate the number of HSPCs needed in each of the 3 pregnancy complication groups. To detect differences in HSPC frequency with a 3 × 4 (group × placental compartment) χ^2 test, we determined that a total sample size of 112 HSPCs was needed to detect a medium effect size of $w = 0.35$, with $\alpha = .05$, and 80% power.[30] To determine differences in HSPC density with a 3 × 4 (group × placental compartment) 2-way analysis of variance (ANOVA), we determined that a total sample size of 118 HSPCs was needed to detect a medium effect size of $f = 0.35$, with $\alpha = .05$, and 80% power.[30] Therefore, we aimed to identify approximately 120 HSPCs (∼40 HSPCs per preterm birth group). Significant main effects detected by χ^2 test or 2-way ANOVA were further analyzed by the Fisher least significant difference test. A P value of <.05 was considered statistically significant. Statistical analyses were done using SPSS statistical software (version 17.0; SPSS Inc, Chicago, Illinois).

Table 1. Sample Characteristics.

	sPTL (n = 6)	PE (n = 6)	iPTL (n = 6)
GA at delivery, mean ± SD, weeks	31.3 ± 1.9	30.3 ± 2.1	28.3 ± 2.7
No. HSPCs identified	49	43	48

Abbreviations: GA, gestational age; HSPC, hematopoietic stem and progenitor cell; iPTL, inflammatory preterm labor; PE, preeclampsia; SD, standard deviation; sPTL, spontaneous preterm labor.

Results

Sample Characteristics

For HSPC localization, placentas from 18 participants were collected (n = 6/group). Gestational ages were not significantly different among the sPTL, PE, and iPTL groups, $F_{(2,15)} = 2.84$, $P = .09$ (Table 1). As planned a priori, a minimum number of 40 HSPCs were identified for each of the 3 groups (Table 1). First- and second-trimester placentas were collected at 5, 6, 9, 12, 16, 17, 21, and 22 weeks of gestation (1 sample per GA).

Hematopoietic Stem and Progenitor Cell Localization: Frequency

A χ^2 test demonstrated a significant relationship between the type of pregnancy complication (sPTL, PE, or iPTL, n = 6 samples per group) and the frequency of HSPCs (n = 43-49 HSPCs per group) within the 4 placental compartments tested (villous small vasculature, villous large vasculature, villous mesenchyme, and chorionic plate), χ^2 (6, N = 140) = 24.45, $P < .001$ (Figure 1A).

At the tissue level, we compared HSPCs in the chorionic plates to the placental villous cores (Figure 1A). In all cases, the cells were more frequently associated with the placental villi ([villi: small vessel] + [villi: large vessel] + [villi: mesenchyme]; sPTL = 87.7%, PE = 79.1%, and iPTL = 77.1%). In the PE and iPTL samples, there was an increased frequency in the chorionic plate (20.9% and 22.9%, respectively) as compared to the control sPTL samples (12.2%), but this was not statistically significant by χ^2 test, χ^2 (2, N = 140) = 2.05, $P = .36$.

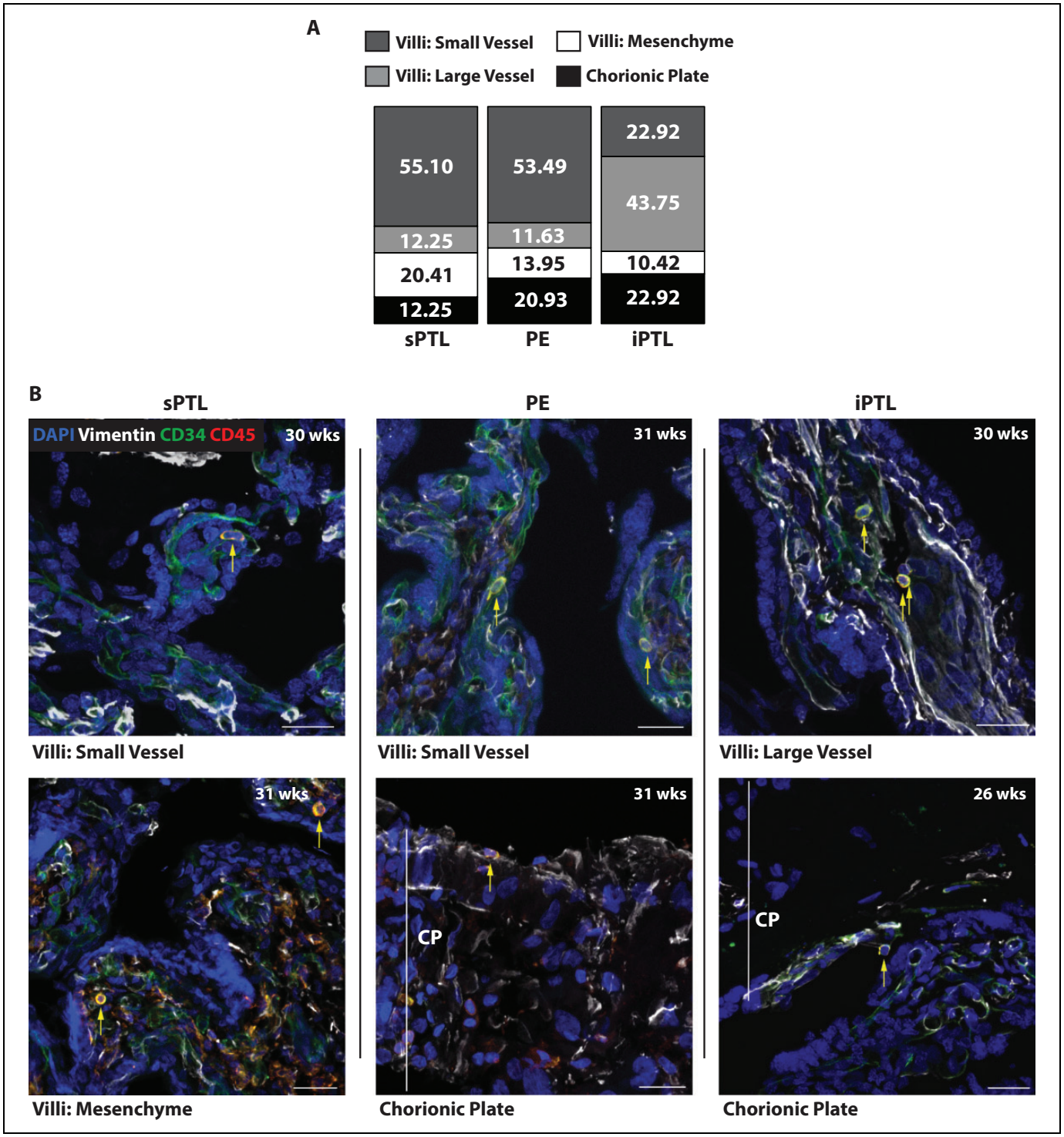

Figure 1. Hematopoietic stem and progenitor cell (HSPC) frequency varied as a function of pregnancy complication and placental compartment. There was a significant relationship between the type of pregnancy complication (spontaneous preterm labor [sPTL], preeclampsia [PE], or inflammatory preterm labor [iPTL]) and the frequency of HSPCs within the 4 placental compartments analyzed (villous small vasculature, villous large vasculature, villous mesenchyme, and chorionic plate [CP]). Hematopoietic stem and progenitor cells immunostained for CD34 and CD45 and identified with a yellow arrow. A, At the tissue level, we compared HSPCs in the CPs to the placental villous cores. In all cases, the cells were more frequently associated with the placental villi. In the PE and iPTL samples, there was an increased frequency in the CP as compared to control sPTL samples, but this was not statistically significant. At the cellular level, within the villous cores, HSPCs in all the groups were distributed between the mesenchymal and endothelial niches. The majority of HSPCs were associated with an endothelial niche. In noninflamed samples, the majority of HSPCs were associated with small vessels. In iPTL samples, there was an increased association with the large vasculature as compared to the sPTL and PE groups. B, Representative images of HSPC immunolocalization. In the sPTL group, HSPCs were most frequently located in the villous small vasculature and villous mesenchyme. In the PE group, HSPCs were most frequently located in the villous small vasculature and CP. In the iPTL group, HSPCs were most frequently located in the villous large vasculature, followed by the CP and villous small vasculature. Scale bars = 25 μm.

At the cellular level, within the villous cores, HSPCs in all the groups were distributed between the mesenchymal and endothelial niches. The majority of HSPCs (~ two-thirds) were associated with an endothelial niche ([villi: small vessel] + [villi: large vessel]; sPTL = 67.3%, PE = 65.1%, and iPTL = 66.7%). In noninflamed samples, the majority of HSPCs were associated with small vessels (defined as ≤2 cell widths in diameter; sPTL = 55.1%, PE = 53.5% vs iPTL = 22.9%). In iPTL samples, there was an increased association with the large vasculature (43.8%) as compared to the sPTL (12.2%) and PE (11.6%) groups. Thus, iPTL was associated with shifts in the HSPC niche within the villi, which were statistically significant by χ^2 test, χ^2 (4, N = 114) = 22.98, $P < .001$. Representative images of HSPC localization are shown in Figure 1B. Additional representative images of HSPCs in each placental compartment and for each pregnancy complication are shown in Figure S1.

A small percentage of HSPCs resided in a mesenchymal niche in the villous core (sPTL = 20.4%, PE = 14.0%, and iPTL = 10.4%), with the majority detected within the vascular space (see above). This is in contrast to the chorionic plate, where cells resided almost entirely within the mesenchymal compartment (78%-83% for all groups, data not shown) and rarely associated with the vasculature. This suggested that the vessels and mesenchyme in the chorionic plate differed from these regions of the villi in terms of their ability to support HSPCs.

Hematopoietic Stem and Progenitor Cell Localization: Density

The HSPC density (percentage of nucleated cells) was significantly affected by the type of pregnancy complication (sPTL, PE, or iPTL, n = 6 samples per group) and the location within the 4 placental compartments tested (villous small vasculature, villous large vasculature, villous mesenchyme, and chorionic plate), $F_{(11,86)} = 4.73$, $P < .001$, partial $\eta^2 = .38$.

The type of pregnancy complication had a significant effect on HSPC density, $F_{(2,86)} = 3.50$, $P < .05$, partial $\eta^2 = .08$. In Figure 2, bars for overall density represented the combined HSPC percentage in the chorionic plate and villous compartments, with a separate bar for each of the 3 pregnancy complications (sPTL, PE, and iPTL). Regardless of the placental location, the overall HSPC density in all compartments combined was significantly higher in the PE and iPTL specimens compared to the sPTL samples (both $P < .05$; Figure 2). There was no significant difference in HSPC density between the PE and iPTL samples ($P = .80$; Figure 2).

The location within either the chorionic plate or the villi also had a significant effect on HSPC density, $F_{(3,86)} = 11.75$, $P < .001$, partial $\eta^2 = .29$. Regardless of the type of pregnancy complication, HSPC density was significantly greater in the chorionic plate as compared to the 3 placental villous compartments (each $P < .001$; Figure 2). Within the chorionic plate, the PE and iPTL samples had increased HSPC density compared to the sPTL samples, but this interaction effect between the location within the placenta and the type of pregnancy complication was not statistically significant, $F_{(6,86)} = 1.84$, $P = .10$, partial $\eta^2 = .11$ (Figure 2).

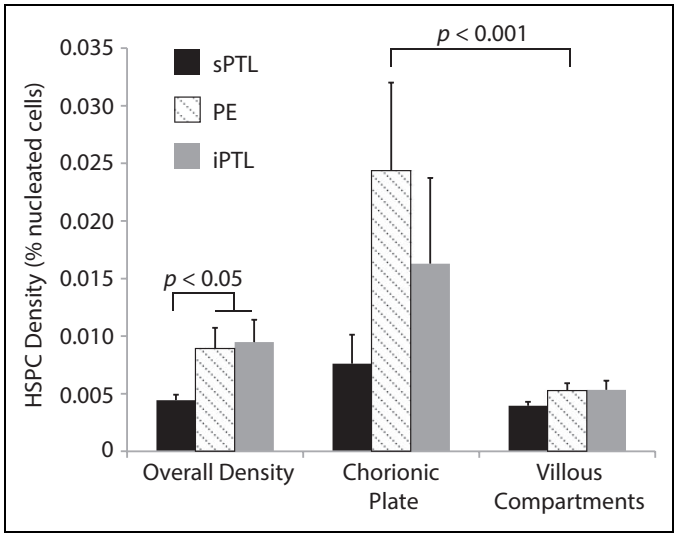

Figure 2. Hematopoietic stem and progenitor cell (HSPC) density varied as a function of pregnancy complication and placental compartment. The HSPC density (percentage of nucleated cells ± standard error of the mean [SEM]) was significantly affected by the type of pregnancy complication (spontaneous preterm labor [sPTL], preeclampsia [PE], or inflammatory preterm labor [iPTL]) and the location within the 4 placental compartments tested (villous small vasculature, villous large vasculature, villous mesenchyme, and chorionic plate). Bars for overall density represented the combined HSPC percentage in the chorionic plate and villous compartments, with a separate bar for each of the 3 pregnancy complications. Overall, the HSPC density was significantly higher in PE and iPTL as compared to sPTL samples. There was no significant difference in HSPC density between the PE and iPTL samples. Additional analyses showed that HSPC density varied by location, for example, the chorionic plate versus the villous compartment. In every case, HSPC density was significantly greater in the chorionic plate as compared to the villous compartments. Within the chorionic plate, the PE and iPTL samples tended toward increased HSPC density compared to the sPTL samples, but this interaction effect did not reach statistical significance. There was no significant difference among pregnancy complications in HSPC density within the villous compartments.

There were no significant differences in HSPC density within each of the 3 villous compartments, including the villous mesenchyme versus the villous large vasculature ($P = .80$), the villous mesenchyme versus the villous small vasculature ($P = .88$), or the villous large vasculature versus the villous small vasculature ($P = .88$; Figure S2). Within the villous compartments, there was a trend toward increased HSPC density in the large vasculature of iPTL samples compared to sPTL and PE samples (Figure S2), which was reminiscent of the effect of iPTL on HSPC frequency (Figure 1).

Placental RUNX1 Expression

RNA-seq data generated from human chorionic villi and smooth chorion samples (n = 2/sample type and trimester)

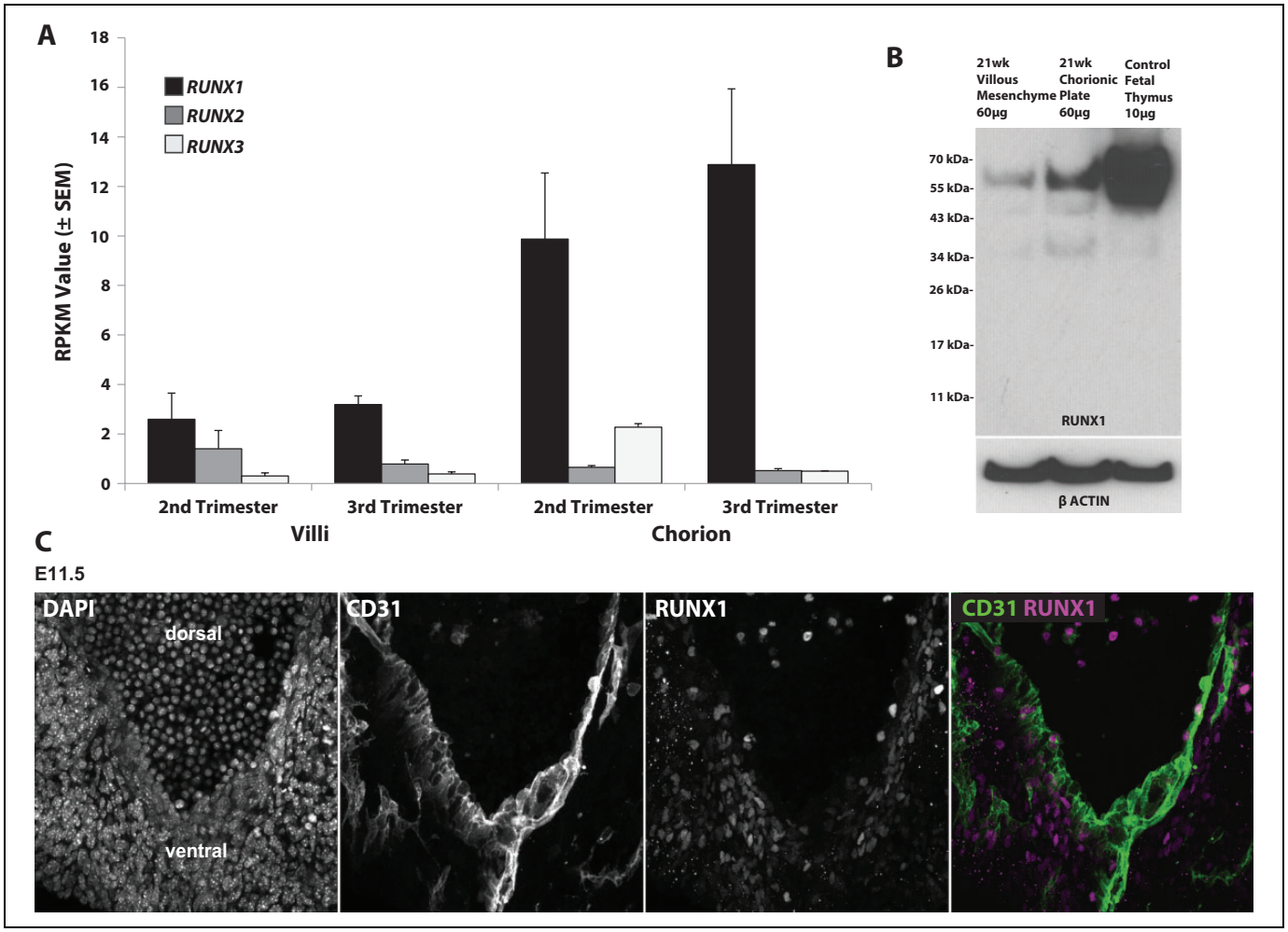

Figure 3. *RUNX1* messenger RNA (mRNA) and RUNX1 protein expression were detected in association with various compartments of the human placenta. A, RNA-seq data generated from human chorionic villi and smooth chorion samples showed predominantly *RUNX1* (vs *RUNX2* or *RUNX3*) RNA expression, which was highest in the chorion where levels rose between second and third trimesters. *RUNX2* and *RUNX3* expression was minimal (≤2 reads per kilobase of transcript per million mapped reads [RPKM]). B, A RUNX1 antibody was used to probe blots of electrophoretically separated control samples (second-trimester human fetal thymocytes) together with lysates of human placental villous mesenchyme and chorionic plate (21 weeks gestational age [GA]). A 59-kDa band was common to the control and placental samples. Other low-molecular-weight isoforms, in all the lysates, reacted less intensely with the antibody. C, The reactivity of this antibody was evaluated on tissue sections of mouse aorta at E11.5. The results showed staining of cell aggregates within the vessel wall, presumably hematopoietic stem cells (HSCs). Endothelial cells were positive for CD31. Nuclei were stained with 4′ 6-diamidino-2-phenylindole (DAPI). Scale bar = 20 μm.

processed in our laboratory as part of the NIH Roadmap Epigenomics Consortium[29] showed predominant *RUNX1* (vs *RUNX2* or *RUNX3*) RNA expression, which was highest in the chorion where levels rose between second and third trimesters (Figure 3A). The expression of *RUNX2* and *RUNX3* was minimal (≤2 reads per kilobase of transcript per million mapped reads [RPKM]). Thus, we used the RUNX1 antibody to probe blots of electrophoretically separated control samples (second-trimester human fetal thymocytes) together with lysates of human villous mesenchyme and chorionic plates (21 weeks GA). A 59-kDa band was common to control and placental samples (Figure 3B). Other low-molecular-weight isoforms, in all the lysates, reacted less intensely with the antibody. Additionally, the reactivity of this antibody was evaluated on tissue sections of mouse aorta at E10.5 (data not shown) and E11.5 (Figure 3C). The results showed staining of cell aggregates within the vessel wall, presumably HSCs. In accord with this result, RUNX1 immunoreactivity was reported in association with the embryonic human aorta and other hemogenic vascular sites.[23]

In additional experiments, we used the same RUNX1 antibody to immunolocalize reactive cells in placentas of various GAs from the embryonic period (<9 weeks GA; Figure 4) through the fetal stage (≥9 weeks GA; Figure 5) of development. Nuclear RUNX1 was identified in our earliest samples at 5 to 6 weeks of gestation (n = 2; Figure 4 and Figure S3). Expression was localized to extravillous cytotrophoblasts (Figure 4A-B). We profiled the mean fluorescence intensity

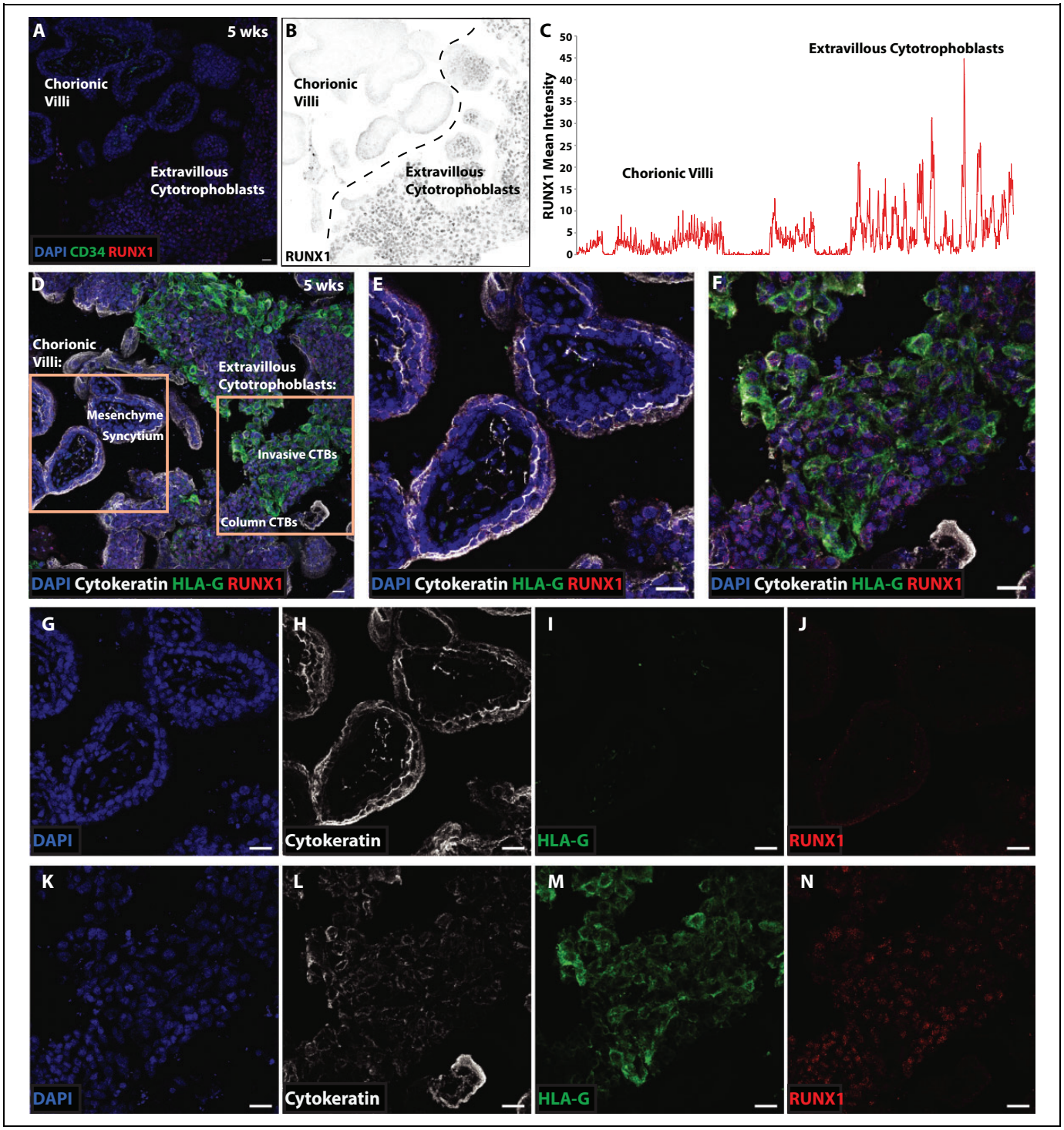

Figure 4. During the embryonic period, extravillous cytotrophoblasts expressed RUNX1. A, Merged 3-color image of DAPI, CD34, and RUNX1 staining of the maternal–fetal interface at 5 weeks of gestation. B, Black and white image of the RUNX1 staining in panel A. Nuclear RUNX1 expression was localized to extravillous cytotrophoblasts that emigrated from the chorionic villi. C, Profiling the mean fluorescence intensity of RUNX1 immunostaining confirmed increased intensity in the extravillous cytotrophoblasts as compared to the villi, which exhibited a low level of nonnuclear background immunoreactivity. D, Colocalization of RUNX1 with HLA-G, whose expression is detected in association with extravillous cytotrophoblasts in columns and within the uterine wall. Cytokeratin staining identified all the trophoblast populations and 4′ 6-diamidino-2-phenylindole (DAPI) staining, the nuclei. The section encompassed floating chorionic villi (left box, enlarged in E) as well as cytotrophoblast columns and invasive cytotrophoblasts within the uterine wall (right box, enlarged in F). Visualization of the individual channels enabled a clearer depiction of the staining patterns of chorionic villi (G-J) and extravillous cytotrophoblasts (K-N). We failed to detect HLA-G or RUNX1 expression in association with floating chorionic villi (E, I, and J). Cytotrophoblasts in the distal portions of cell columns and within the uterine wall immunostained with anti-HLA-G (F and M). RUNX1 was expressed, in a nuclear pattern, throughout the columns and by cytotrophoblasts inside the uterine wall (F and N). Scale bars = 25 μm.

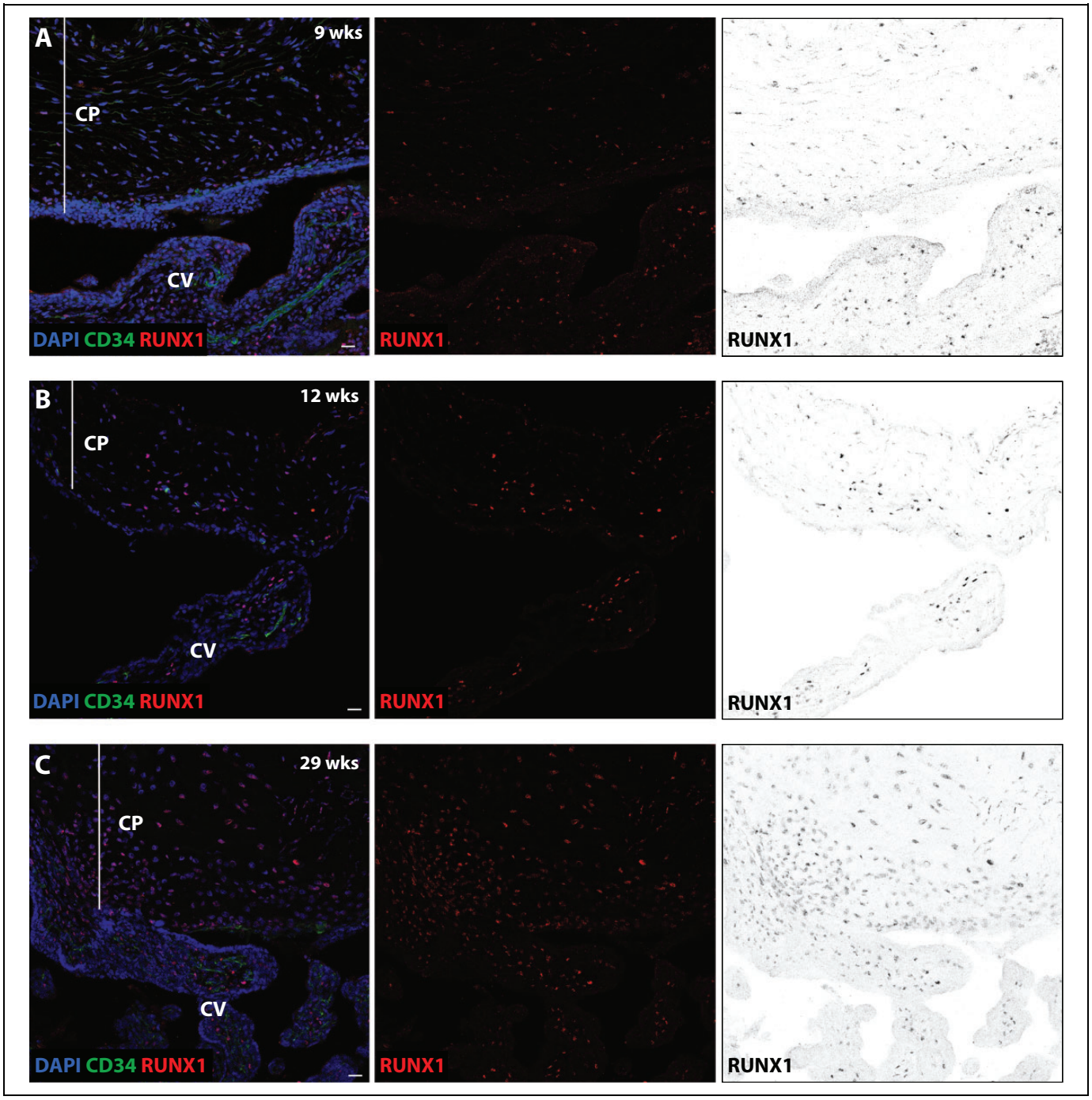

Figure 5. During the fetal period, RUNX1 was expressed by cells of the chorionic plate (CP) and mesenchymal cores of chorionic villi (CV). Samples were analyzed in the fetal period (9-34 weeks of gestational age [GA]). Representative images from samples at (A) 9 weeks GA, (B) 12 weeks GA, and (C) 29 weeks GA. Left panels, merged color image of DAPI, CD34, and RUNX1 immunostaining. Middle panels, image of RUNX1 immunostaining in red. Right panels, image of RUNX1 immunostaining in black. Scale bars = 25 μm.

of RUNX1 across Figure 4A and confirmed increased intensity in the extravillous cytotrophoblasts as compared to the villi, which exhibited a low level of nonnuclear background immunoreactivity (Figure 4C).

Next, we colocalized RUNX1 with Human Leukocyte Antigen G (HLA-G), which is detected in association with cytotrophoblasts in columns and within the uterine wall.[31] Cytokeratin staining identified all the trophoblast populations and DAPI staining, the nuclei. An example of the results is shown in Figure 4D. The sections encompassed floating chorionic villi (left box; enlarged in Figure 4E) as well as cytotrophoblast columns and invasive cytotrophoblasts within the uterine wall (right box; enlarged in Figure 4F). Visualization of the individual channels enabled a clearer depiction of the

staining patterns of the chorionic villi (Figure 4G-J) and extravillous cytotrophoblasts (Figure 4K-N). We failed to detect HLA-G or RUNX1 expression in association with floating chorionic villi (Figure 4E, I, and J). As expected, cytotrophoblasts in the distal portions of cell columns and within the uterine wall immunostained with anti-HLA-G (Figure 4F and M). RUNX1 was expressed, in a nuclear pattern, throughout the columns and by cytotrophoblasts inside the uterine wall (Figure 4F and N). This pattern of RUNX1 immunoreactivity in extravillous cytotrophoblasts was maintained in the second and third trimesters of pregnancy (data not shown).

We also immunolocalized RUNX1 in the regions where we detected HSPCs. Because the chorionic plate is not well developed during the embryonic period, we examined samples in the fetal period from 9 weeks through 34 weeks of GA (normal pregnancies at 9, 12, and 16 weeks of GA, n = 3 total; sPTL, n = 5; PE, n = 5; iPTL n = 5). RUNX1 was expressed in the chorionic plate, the mesenchymal cores of chorionic villi (Figure 5A-C), and very infrequently within the $CD34^+$ vessels (data not shown).

Next, we examined the effects of pregnancy complications on RUNX1 expression in the placenta. The patterns were similar among the 3 pregnancy complication groups. However, compared to noninflamed samples (sPTL, n = 5, Figure 6A and B; PE, n = 5, Figure 6C and D), the iPTL samples (n = 5, Figure 6E and F) had increased numbers of $RUNX1^+$ cells within the vessel lumens, $F_{(2,19)} = 12.77$, $P < .001$, partial $\eta^2 = .57$. There was no difference between the sPTL and PE samples in the number of intraluminal $RUNX1^+$ cells ($P = .904$). These intraluminal $RUNX1^+$ cells were heterogeneous in their coexpression of CD34 (43%-63% of intraluminal $RUNX1^+$ cells were also $CD34^+$; Figure 6G).

One of the 6 iPTL samples (GA = 26 weeks) contained multiple $RUNX1^+$ cell clusters (Figure 7A) in arteries and veins. Some were associated with the endothelial vessel wall (Figure 7B), which we identified as arterial in a serial section stained with SOX17 (Figure 7C). This transcription factor works upstream of the Notch pathway to induce arterial specification and is expressed in arterial endothelial cells from the embryonic period into adulthood.[32] We validated the SOX17 arterial specificity in human tissue using a 22-week GA umbilical cord sample in which arterial and venous identities were confirmed by gross visual inspection (n = 1; Figure S4). Upon closer examination, other areas of clustered $RUNX1^+$ cells, in the same sample, were heterogeneous with regard to their CD34 expression as well as their nuclear morphology (Figure 7D). This finding is congruent with the heterogeneous $RUNX1^+$ cell clusters previously described in mouse dorsal aorta.[18]

Discussion

Hematopoietic stem and progenitor cells were rare cell types in the placenta, making up <1% of nucleated cells identified by microscopy. The fact that HSPCs were more likely to be found in the placental villous compartment compared to the chorionic plate is congruent with our laboratory's previous analyses by flow cytometry, which showed that (on average) there were 10 times more $CD34^{++}CD45^{low}$ HSCs in the placental villi than in the chorionic plate.[5] Although HSPCs occurred at a decreased frequency in the chorionic plate compared to the placental villi, these cells were present at significantly higher densities in this location. This finding suggests that the second- and third-trimester chorionic plate and placental villi are sources of HSPCs. The increased HSPC density in the chorionic plate was exaggerated in the PE and iPTL samples, although this was not statistically significant. Located just beneath the amnion layer that is devoid of HSPCs,[5] the chorionic plate, which is in close contact with the fetal compartment, is an important barrier in the immune defense of the fetus. We speculate that increasing densities of HSPCs at this barrier in the setting of PE or iPTL may fuel the development of mature immune cells such as macrophage-like Hofbauer cells, which are in abundance in the placenta, or red blood cells to improve oxygenation.[7] Erythroid and macrophage cell types have also been recently demonstrated to either develop de novo or differentiate within placental compartments.[33]

At the microenvironmental level, we identified HSPCs in both mesenchymal and endothelial niches but determined that they are predominantly associated with the vascular endothelium. This is congruent with placental studies in mice, where the vascular endothelium also serves as an important niche for HSCs.[6,34] Also in mice, HSC emergence is noted from the ventral portion of the dorsal aorta within the aorta–gonad–mesonephros (AGM) region, the vitelline artery, and the umbilical artery,[18,35] as well as the large vessels of the placenta.[6] The smaller vasculature in the mouse placenta provides a supportive niche for hematopoietic cell proliferation/expansion.[6] The shift in the HSPC villous niche from the small to the large vasculature in the iPTL samples suggested different functional roles for these niches in the human placenta, as well, which may be affected by pregnancy complications. Further studies are needed to determine whether human placental endothelial cells regulate HSCs using cytokine and chemokine signaling pathways similar to those described in mice.[34]

We demonstrate the novel finding of *RUNX1* RNA expression as determined by RNA-seq (second and third trimesters) and RUNX1 protein expression as determined by immunoblot (second trimester) and immunolocalization (first through third trimesters) in the human placenta. *Runx1* placental RNA expression has previously been identified by reverse transcription-polymerase chain reaction in mice.[36] Although we cannot rule out RUNX2 or RUNX3 expression with the antibody used, we believe this represents RUNX1-specific expression in the placenta. All have similar predicted molecular weights (RUNX1: 49 kDa, RUNX2: 56 kDa, RUNX3: 44 kDa; Abcam). RUNX2 (AML3) is a transcription factor involved in osteoblastic differentiation and skeletal morphogenesis.[37] RUNX3 (AML2) plays a role in the development of the gastrointestinal system,[38] dorsal root ganglia,[39] and the hematopoietic system.[40] There is some degree of overlap between RUNX3 and RUNX1 expression in the hematopoietic

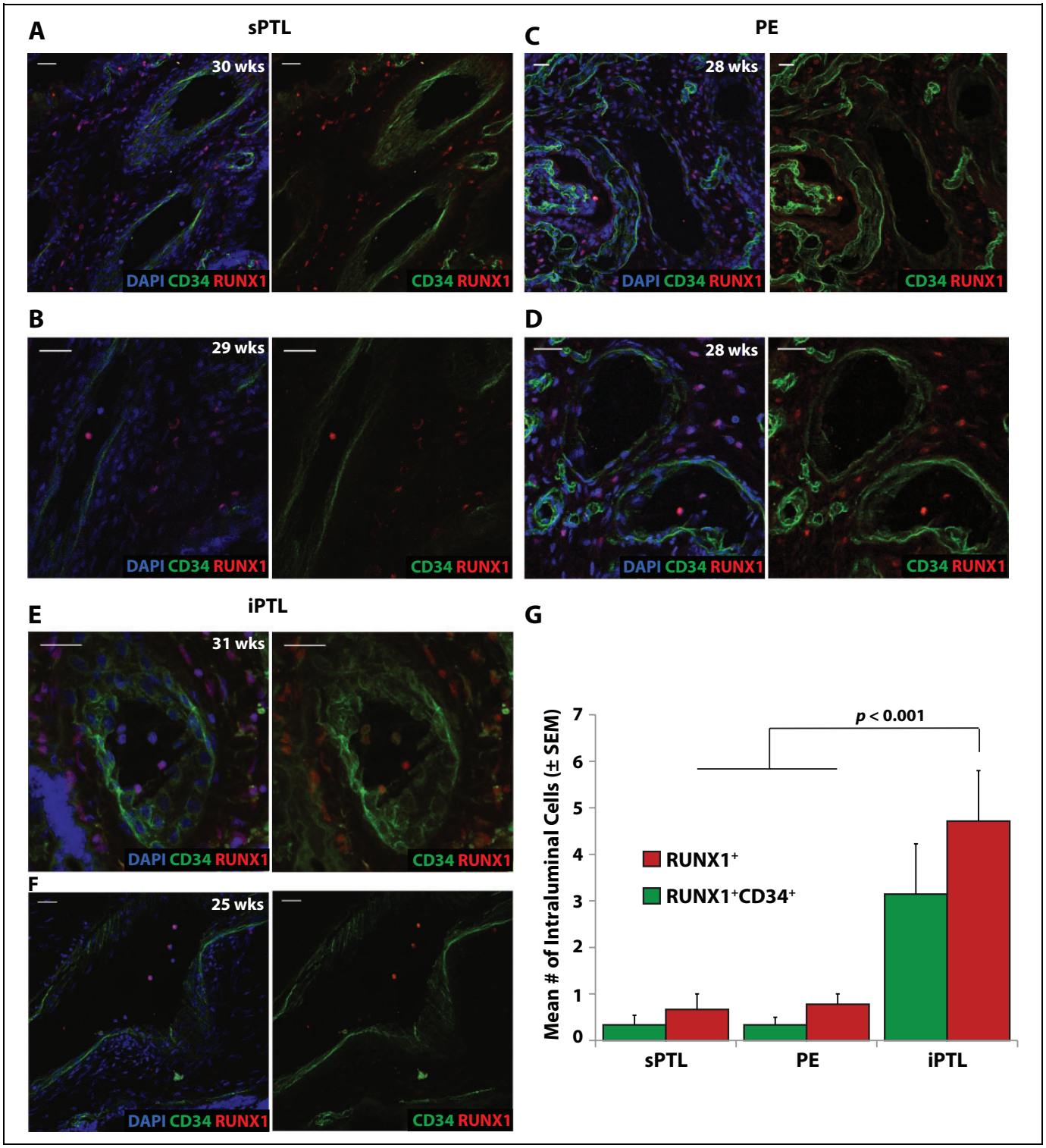

Figure 6. Preterm labor in the setting of inflammation was associated with increased numbers of RUNX1$^+$ cells within the placental vessels. A-F, (Left) A merged 3-color image of 4′ 6-diamidino-2-phenylindole (DAPI), CD34, and RUNX1 staining and (right) a merged 2-color image of CD34 and RUNX1 immunolocalization. A, A representative image of a spontaneous preterm labor (sPTL) sample at 30 weeks gestational age (GA). B, A representative image of an sPTL sample at 29 weeks GA. C and D, Representative images of a preeclampsia (PE) sample at 28 weeks GA. E, A representative image of an inflammatory preterm labor (iPTL) sample at 31 weeks GA. F, A representative image of an iPTL sample at 25 weeks GA. G, The mean number of intraluminal RUNX1$^+$ cells (red bars) was significantly higher in iPTL as compared to sPTL and PE samples. More than half (43%-63%) of intraluminal RUNX1$^+$ cells were also CD34$^+$ (green bars). Scale bars = 25 μm.

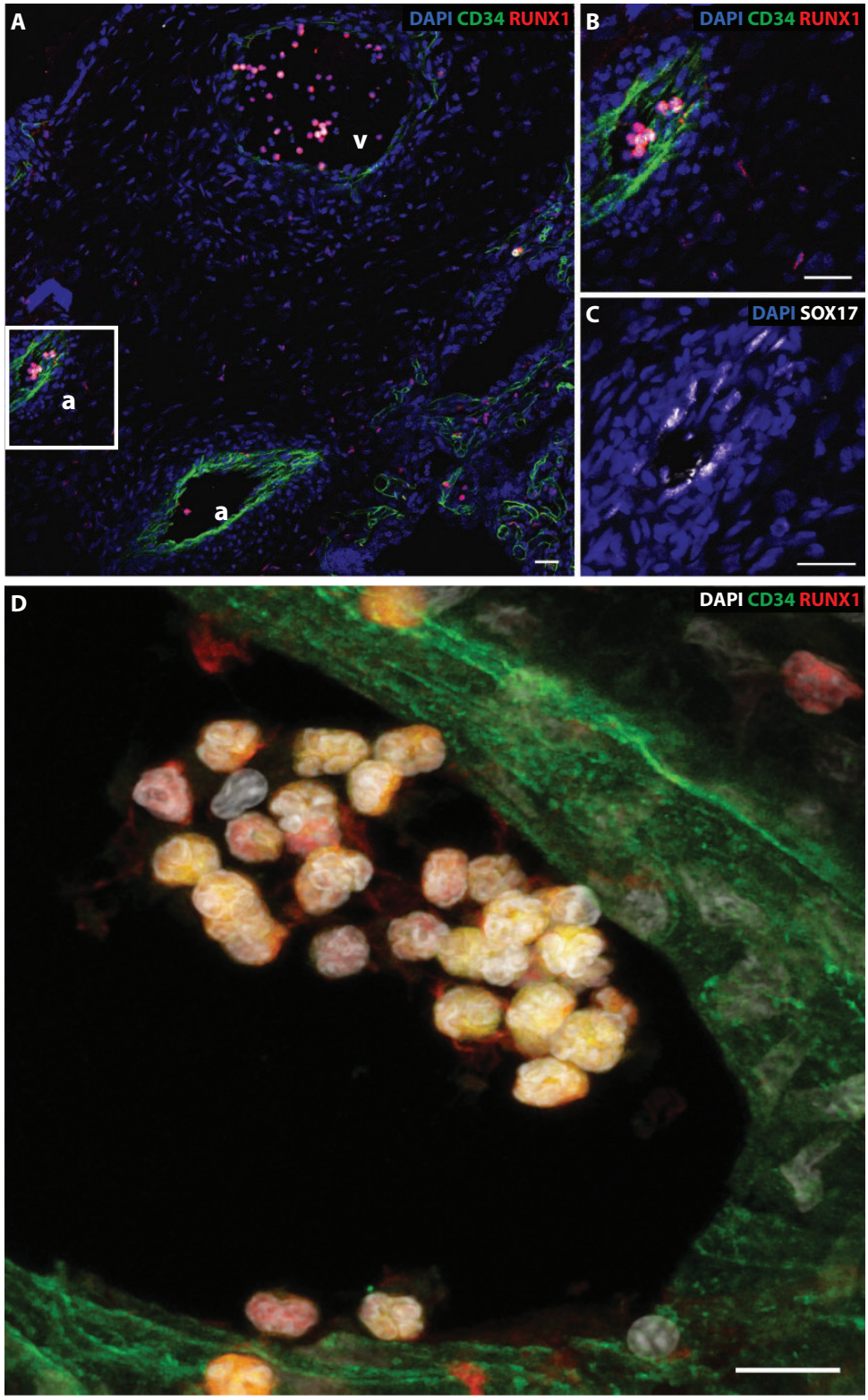

Figure 7. A 26 weeks gestational age (GA) inflammatory preterm labor (iPTL) placenta had multiple RUNX1^{+} cell clusters in the vessels. A, RUNX1^{+} cell clusters in arteries (a) and veins (v). B, Some were associated with the endothelial vessel wall, (C) which we identified as arterial in a serial section stained with SOX17. D, At higher magnification, other areas of clustered RUNX1^{+} cells, in the same sample, were heterogeneous with regard to their CD34 expression and nuclear morphology (D). Scale bars, A to C = 25 μm; D = 10 μm.

system, although RUNX3 is not found in the dorsal aorta of mice.[41] An immunopositive band likely representing RUNX1 was noted near the expected molecular weight of 49 kDa the second-trimester samples examined (Figure 3B). The identity of the additional bands of lower intensity is unclear, but they may be isoforms of this molecule, which have previously been reported.[42] To support our hypothesis of RUNX1 expression in the human placenta, we stained a 28-week PE sample with a RUNX1-specific antibody (Abcam 35962; Figure 6C). The results showed a similar expression pattern to the RUNX antibody used in our other experiments (Abcam 92336b; Figure 6D). In addition, RNA expression of *RUNX2* and *RUNX3* was minimal ($\leq$2 RPKM by RNA-seq) in second- and third-trimester samples (Figure 3A).

It is interesting that RUNX1 localized to extravillous cytotrophoblasts in the early embryonic period, given the important role of these cells in placental vascular remodeling. Invasive cytotrophoblasts replace endothelial cells and perivascular smooth muscle cells early in gestation to allow for sufficient placental perfusion and exchange of nutrients at the maternal–fetal interface.[43] Previously, we showed that this cytotrophoblast subpopulation expresses many endothelial-type molecules,[44] and here, we add RUNX1 to this list.

Placental and chorionic mesenchyme may be supportive of endothelial hematopoietic activity as has been noted at other vascular hemogenic sites. At the onset of the fetal period of development (starting at 9 weeks of GA), RUNX1 localized primarily to the mesenchyme of the chorionic plate and of the placental villous core and very infrequently to the vascular endothelium. We and others[20,25] have previously shown that in mice, RUNX1$^+$ cells are present in both the aortic endothelium and subaortic mesenchyme. Through fate-tracing experiments, we demonstrated that the aortic endothelium has HSC activity, but later subaortic mesenchyme does not.[45] Interestingly, an earlier mesenchymal population did transiently contribute to the endothelium and subsequent HSC activity in the aorta, yolk sac, and placenta, but this did not persist in later mesenchyme.[45] Data from chick embryos demonstrated that mesenchyme was required for the formation of RUNX1$^+$ cells and hematopoietic cell clusters, but was not itself a source of HSCs, supporting the hypothesis that mesenchyme creates a microenvironment that is favorable for hematopoiesis from hemogenic endothelium.[46] We propose that HSPCs may originate from placental hematopoietic niches comprised RUNX1$^+$ mesenchyme and vascular endothelium.

Our observations of placental HSPCs in direct contact with endothelial cells and the presence of RUNX1$^+$ clusters in arterial vessels within the midgestation placenta indicate that hemogenic endothelium may be active at later stages of human fetal development. In contrast, RUNX1$^+$ cell clusters representing definitive HSCs[18,20,47] emerge from the endothelium of the mouse embryonic AGM region during a specific developmental window, E10-E12,[35] as demonstrated by live imaging techniques.[48] Transient clusters of HSPCs emerging from hemogenic endothelium are also present in human aorta between about 6 and 8 weeks of GA (4-6 weeks postconceptual age).[23,49] Our findings suggest that an increased window of opportunity for endothelial-to-hematopoietic expansion may exist in human placenta, particularly in the inflamed state.

Our results support the hypothesis that inflammation may positively regulate placental/chorionic hematopoiesis. The iPTL samples had an increased intraluminal predominance of RUNX1$^+$ cells, as well as an increased frequency and density of HSPCs in the large vasculature, suggesting increased HSPC mobilization into circulation in the setting of inflammation. Currently, we are pursuing this hypothesis with further studies of umbilical cord blood HSPCs. Hematopoietic stem cells can respond directly to inflammatory cytokines.[50,51] It is also becoming increasing apparent that inflammatory processes (via tumor necrosis factor α and interferon γ) are involved in early HSC emergence in the developing embryo, even in nonpathological states.[52-55] An increase in HSPC production may represent an advantageous evolutionary response for preterm neonates, as higher HSPC levels in this population are associated with lowered risk for common morbidities of prematurity including intraventricular hemorrhage, respiratory distress syndrome, anemia, and infection.[56] Although we know that HSCs are produced endogenously in the placenta,[6] it remains unclear how much of a contribution this site has to hematopoiesis relative to the liver. In mice, the placental HSC contribution is significant at midgestation, with expansion occurring prior to and overlapping that of fetal liver HSCs, and before the appearance of large numbers of circulating HSCs.[57]

In addition to term placentas, preterm placentas and chorionic plates are untapped reservoirs of HSPCs that could be utilized in conjunction with umbilical cord blood stem cells for transplantation purposes. The identification of a predominantly endothelial niche in the placenta suggests that HSPC isolation methods utilizing placental perfusion may be optimal. We believe that the heterogeneous etiologies of preterm birth may differentially affect HSPC development and that continued investigation is necessary. Hematopoietic stem and progenitor cells from preterm cord blood samples have increased functional clonogenic potential compared to term HSPCs, suggesting their possible increased therapeutic potential.[56,58] In the future, we will determine whether this is also true for placental HSPCs. The evidence for the possible persistence of hemogenic endothelium in the inflamed placenta has important implications for future attempts to initiate or expand definitive, transplantable HSCs from placental tissue ex vivo. An understanding of both umbilical and placental HSPCs in preterm neonates has critical implications for the use of autologous stem cell therapy in the preterm population.

Acknowledgements

The authors thank Alan Gutierrez for his technical assistance with immunohistochemistry protocols. The authors are also grateful to Stephanie Leong and Jason Farrell for study enrollment and specimen collection and to Dr Trevor Burt's laboratory for providing the thymus tissue utilized for immunoblotting.

Declaration of Conflicting Interests

The author(s) declared no potential conflicts of interest with respect to the research, authorship, and/or publication of this article.

Funding

The author(s) disclosed receipt of the following financial support for the research, authorship, and/or publication of this article: This work was supported by the National Institutes of Health, R01 HD076253-01 (S.J.F.) and 5T32HD071860-04 (K.L.P.), the Netherlands KWF Fellowship (F.L.B.), the Burroughs Wellcome Fund Career Award for Medical Scientists (A.C.Z., 1008408.01), and the California Institute for Regenerative Medicine (A.C.Z., RN3-06479).

Supplemental Material

The online supplemental figures and tables are available at http://rs.sagepub.com/supplemental.

References

1. Barcena A, Muench MO, Kapidzic M, Fisher SJ. A new role for the human placenta as a hematopoietic site throughout gestation. *Reprod Sci*. 2009;16(2):178-187.
2. Robin C, Bollerot K, Mendes S, et al. Human placenta is a potent hematopoietic niche containing hematopoietic stem and progenitor cells throughout development. *Cell Stem Cell*. 2009;5(4):385-395.
3. Serikov V, Hounshell C, Larkin S, et al. Human term placenta as a source of hematopoietic cells. *Exp Biol Med (Maywood)*. 2009;234(7):813-823.
4. Ivanovs A, Rybtsov S, Welch L, Anderson RA, Turner ML, Medvinsky A. Highly potent human hematopoietic stem cells first emerge in the intraembryonic aorta-gonad-mesonephros region. *J Exp Med*. 2011;208(12):2417-2427.
5. Barcena A, Muench MO, Kapidzic M, Gormley M, Goldfien GA, Fisher SJ. Human placenta and chorion: potential additional sources of hematopoietic stem cells for transplantation. *Transfusion*. 2011;51(suppl 4):94S-105S.
6. Rhodes KE, Gekas C, Wang Y, et al. The emergence of hematopoietic stem cells is initiated in the placental vasculature in the absence of circulation. *Cell Stem Cell*. 2008;2(3):252-263.
7. Bárcena A, Muench MO, Kapidzic M, Gormley M, Fisher SJ. The human term placenta as a source of transplantable hematopoietic stem cells. In: Atala A, Murphy SV, eds. *Perinatal Stem Cells*. New York: Springer-Verlag; 2014:171-182.
8. Tita AT, Andrews WW. Diagnosis and management of clinical chorioamnionitis. *Clin Perinatol*. 2010;37(2):339-354.
9. Zipursky A, Palko J, Milner R, Akenzua I. The hematology of bacterial infections in premature infants. *Pediatrics*. 1976;57(6):839-853.
10. Nittala S, Subbarao GC, Maheshwari A. Evaluation of neutropenia and neutrophilia in preterm infants. *J Matern Fetal Neonatal Med*. 2012;25(suppl 5):100-103.
11. Borzychowski AM, Sargent IL, Redman CW. Inflammation and pre-eclampsia. *Semin Fetal Neonatal Med*. 2006;11(5):309-316.
12. Chaiworapongsa T, Chaemsaithong P, Yeo L, Romero R. Pre-eclampsia part 1: current understanding of its pathophysiology. *Nat Rev Nephrol*. 2014;10(8):466-480.
13. Fraser SH, Tudehope DI. Neonatal neutropenia and thrombocytopenia following maternal hypertension. *J Paediatr Child Health*. 1996;32(1):31-34.
14. Neufeld MD, Frigon C, Graham AS, Mueller BA. Maternal infection and risk of cerebral palsy in term and preterm infants. *J Perinatol*. 2005;25(2):108-113.
15. Shevell A, Wintermark P, Benini R, Shevell M, Oskoui M. Chorioamnionitis and cerebral palsy: lessons from a patient registry. *Eur J Paediatr Neurol*. 2014;18(3):301-307.
16. Kumar R, Yu Y, Story RE, et al. Prematurity, chorioamnionitis, and the development of recurrent wheezing: a prospective birth cohort study. *J Allergy Clin Immunol*. 2008;121(4):878-884.e876.
17. Barker DJ. The developmental origins of adult disease. *Eur J Epidemiol*. 2003;18(8):733-736.
18. North TE, de Bruijn M, Stacy T, et al. Runx1 expression marks long-term repopulating hematopoietic stem cells in the midgestation mouse embryo. *Immunity*. 2002;16(5):661-672.
19. Uhlénm M, Fagerberg L, Hallström BM, et al. Tissue-based map of the human proteome. *Science*. 2015;347(6220):1260419.
20. North T, Gu T-L, Stacy T, et al. Cbfa2 is required for the formation of intra-aortic hematopoietic clusters. *Development*. 1999;126(11):2563-2575.
21. Chen MJ, Yokomizo T, Zeigler BM, Dzierzak E, Speck NA. Runx1 is required for the endothelial to haematopoietic cell transition but not thereafter. *Nature*. 2009;457(7231):887-891.
22. Zape JP, Zovein AC. Hemogenic endothelium: origins, regulation, and implications for vascular biology. *Semin Cell Dev Biol*. 2011;22(9):1036-1047.
23. Bos FL, Hawkins JS, Zovein AC. Single-cell resolution of morphological changes in hemogenic endothelium. *Development*. 2015;142(15):2719-2724.
24. Tober J, Yzaguirre AD, Piwarzyk E, Speck NA. Distinct temporal requirements for Runx1 in hematopoietic progenitors and stem cells. *Development*. 2013;140(18):3765-3776.
25. Ottersbach K, Dzierzak E. The murine placenta contains hematopoietic stem cells within the vascular labyrinth region. *Dev Cell*. 2005;8(3):377-387.
26. Herron MA, Katz M, Creasy RK. Evaluation of a preterm birth prevention program: preliminary report. *Obstetr Gynecol*. 1982;59(4):452-456.
27. Zhou Y, Bianco K, Huang L, et al. Comparative analysis of maternal-fetal interface in preeclampsia and preterm labor. *Cell Tissue Res*. 2007;329(3):559-569.
28. Rasband WS. ImageJ. Bethesda, MD: US National Institutes of Health; 1997-2014.
29. Roadmap Epigenomics Consortium. Kundaje A, Meuleman W, et al. Integrative analysis of 111 reference human epigenomes. *Nature*. 2015;518(7539):317-330.
30. Faul F, Erdfelder E, Lang A-G, Buchner A.G*Power 3: a flexible statistical power analysis program for the social, behavioral, and biomedical sciences. *Behav Res Methods*. 2007;39(2):175-191.
31. McMaster MT, Librach CL, Zhou Y, et al. Human placental HLA-G expression is restricted to differentiated cytotrophoblasts. *J Immunol*. 1995;154(8):3771-3778.

32. Corada M, Orsenigo F, Morini MF, et al. Sox17 is indispensable for acquisition and maintenance of arterial identity. *Nat Commun*. 2013;4:2609.
33. Van Handel B, Prashad SL, Hassanzadeh-Kiabi N, et al. The first trimester human placenta is a site for terminal maturation of primitive erythroid cells. *Blood*. 2010;116(17):3321-3330.
34. Sasaki T, Mizuochi C, Horio Y, Nakao K, Akashi K, Sugiyama D. Regulation of hematopoietic cell clusters in the placental niche through SCF/Kit signaling in embryonic mouse. *Development*. 2010;137(23):3941-3952.
35. de Bruijn MFTR, Speck NA, Peeters MCE, Dzierzak E. Definitive hematopoietic stem cells first develop within the major arterial regions of the mouse embryo. *EMBO J*. 2000;19(11): 2465-2474.
36. Alvarez-Silva M, Belo-Diabangouaya P, Salaun J, Dieterlen-Lievre F. Mouse placenta is a major hematopoietic organ. *Development*. 2003;130(22):5437-5444.
37. Katagiri T, Takahashi N. Regulatory mechanisms of osteoblast and osteoclast differentiation. *Oral Dis*. 2002;8(3):147-159.
38. Li Q, Ito K, Sakakura C, et al. Causal relationship between the loss of RUNX3 expression and gastric cancer. *Cell*. 2002;109(1): 113-124.
39. Levanon D, Bettoun D, Harris-Cerruti C, et al. The Runx3 transcription factor regulates development and survival of TrkC dorsal root ganglia neurons. *EMBO J*. 2002;21(13): 3213-3567.
40. Kalev-Zylinska ML, Horsfield JA, Flores MV, et al. Runx3 is required for hematopoietic development in zebrafish. *Dev Dyn*. 2003;228(3):323-336.
41. Levanon D, Brenner O, Negreanu V, et al. Spatial and temporal expression pattern of Runx3 (Aml2) and Runx1 (Aml1) indicates non-redundant functions during mouse embryogenesis. *Mech Dev*. 2001;109(2):413-417.
42. Montero-Ruiz O, Alcantara-Ortigoza MA, Betancourt M, Juarez-Velazquez R, Gonzalez-Marquez H, Perez-Vera P. Expression of RUNX1 isoforms and its target gene BLK in childhood acute lymphoblastic leukemia. *Leuk Res*. 2012;36(9):1105-1111.
43. Tessier DR, Yockell-Lelievre J, Gruslin A. Uterine spiral artery remodeling: the role of uterine natural killer cells and extravillous trophoblasts in normal and high-risk human pregnancies. *Am J Reprod Immunol*. 2015;74(1):1-11.
44. Fisher SJ. Why is placentation abnormal in preeclampsia? *Am J Obstet Gynecol*. 2015;213(4 suppl):S115-S122.
45. Zovein AC, Hofmann JJ, Lynch M, et al. Fate tracing reveals the endothelial origin of hematopoietic stem cells. *Cell Stem Cell*. 2008;3(6):625-636.
46. Richard C, Drevon C, Canto PY, et al. Endothelio-mesenchymal interaction controls runx1 expression and modulates the notch pathway to initiate aortic hematopoiesis. *Dev Cell*. 2013;24(6): 600-611.
47. Medvinsky A, Rybtsov S, Taoudi S. Embryonic origin of the adult hematopoietic system: advances and questions. *Development*. 2011;138(6):1017-1031.
48. Boisset JC, van Cappellen W, Andrieu-Soler C, Galjart N, Dzierzak E, Robin C. In vivo imaging of haematopoietic cells emerging from the mouse aortic endothelium. *Nature*. 2010;464(7285): 116-120.
49. Tavian M, Coulombel L, Luton D, Clemente HS, Dieterlen-Lievre F, Peault B. Aorta-associated CD34+ hematopoietic cells in the early human embryo. *Blood*. 1996;87(1):67-72.
50. Baldridge MT, King KY, Goodell MA. Inflammatory signals regulate hematopoietic stem cells. *Trends Immunol*. 2011;32(2):57-65.
51. King KY, Goodell MA. Inflammatory modulation of HSCs: viewing the HSC as a foundation for the immune response. *Nat Rev Immunol*. 2011;11(10):685-692.
52. Espin-Palazon R, Stachura DL, Campbell CA, et al. Proinflammatory signaling regulates hematopoietic stem cell emergence. *Cell*. 2014;159(5):1070-1085.
53. Sawamiphak S, Kontarakis Z, Stainier DY. Interferon gamma signaling positively regulates hematopoietic stem cell emergence. *Dev Cell*. 2014;31(5):640-653.
54. Li Y, Esain V, Teng L, et al. Inflammatory signaling regulates embryonic hematopoietic stem and progenitor cell production. *Genes Dev*. 2014;28(23):2597-2612.
55. He Q, Zhang C, Wang L, et al. Inflammatory signaling regulates hematopoietic stem and progenitor cell emergence in vertebrates. *Blood*. 2015;125(7):1098-1106.
56. Kotowski M, Safranow K, Kawa MP, et al. Circulating hematopoietic stem cell count is a valuable predictor of prematurity complications in preterm newborns. *BMC Pediatr*. 2012;12:148-163.
57. Gekas C, Dieterlen-Lievre F, Orkin SH, Mikkola HK. The placenta is a niche for hematopoietic stem cells. *Dev Cell*. 2005;8(3): 365-375.
58. Wisgrill L, Schuller S, Bammer M, et al. Hematopoietic stem cells in neonates: any differences between very preterm and term neonates? *PLoS One*. 2014;9(9):e106717.